Water Scaffolding in Collagen: Implications on Protein Dynamics as Revealed by Solid-State NMR

Abil E. Aliev, Denis Courtier-Murias

Department of Chemistry, University College London, 20 Gordon Street, London WC1H 0AJ, UK

ABSTRACT:

Solid-state NMR studies of collagen samples of various origins confirm that the amplitude of collagen backbone and sidechain motions increases significantly on increasing the water content. This conclusion is supported by the changes observed in three different NMR observables: (i) the line-width dependence on the ^1H decoupling frequency; (ii) ^{13}C CSA changes for the peptide carbonyl groups, and (iii) dephasing rates of ^1H-^{13}C dipolar couplings. In particular, a nearly threefold increase in motional amplitudes of the backbone librations about C-C^α or N-C^α bonds was found on increasing the added water content up to 47 wt%D_2O. On the basis of the frequencies of NMR observables involved, the timescale of the protein motions dependent on the added water content is estimated to be of the order of microseconds. This estimate agrees with that from wideline T_2 ^1H NMR measurements. Also, our wideline ^1H NMR measurements revealed that the timescale of the microsecond motions in proteins reduces significantly on increasing the added water content, i.e., an $\sim$15-fold increase in protein motional frequencies is observed on increasing the added water content to 45 wt% D_2O. The observed changes in collagen dynamics is attributed to the increase in water translational diffusion on increasing the amount of added water, which leads to more frequent "bound water/free water" exchange on the protein surface, accompanied by the breakage and formation of new hydrogen bonds with polar functionalities of protein. © 2013 The Authors Biopolymers Published by Wiley Periodicals, Inc. Biopolymers 101: 246–256, 2014.

Keywords: protein; collagen; water; structure; dynamics; solid-state NMR

INTRODUCTION

Collagen ("glue forming" in Greek) is one of the most abundant proteins in Nature.[1] In particular, it is the most abundant protein in mammals and about a quarter of the total mass of proteins in vertebrates is collagen.[1] The structure of collagen molecule, which is known to be $\sim$3000 Å in length and $\sim$15 Å in diameter, has been described as a triple-helix of three individual protein strands.[2–4] The three helical chains are staggered by one residue, allowing for interchain hydrogen bonds.[2–4] Formation of the triple helix conformation requires the presence of a repeated -Gly-Xaa-Yaa- sequence, the most common sequence being -Gly-Pro-Hyp-.[5] However, other amino acids are also known to occur as Xaa or Yaa, while any amino acid residue with a side chain would be unsuitable to replace Gly in the middle of a triple helix. The molecular weight of collagen is estimated to be $\sim$285,000.[6] The triple-helical collagen molecules associate in a highly regular manner to form fibrils.[7] Because of its large size, the direct structural determination of collagen is complicated. Nevertheless, the X-ray
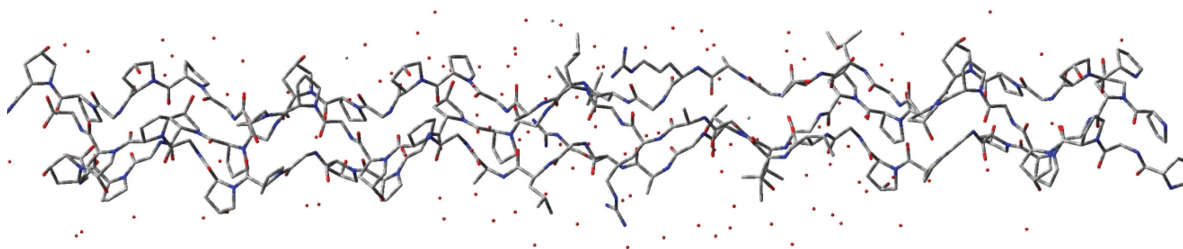
FIGURE 1 An example of the collagen structural analog (PDB entry 1BKV),[9] showing water surrounding of a triple helix in the solid state. Red dots indicate oxygen atoms of water molecules.

diffraction (XRD) data showed that collagen molecules are ordered in the direction parallel to the long axis of the molecule.[2–4] Various XRD studies of structural analogs of collagen have been reported (Figure 1).[8,9] These studies revealed an ordered cylinder of hydration surrounding collagen molecules. It has been shown that the triple-helical structure causes more ordering of the hydration water than the denaturated single polipeptide chains.[10]

The molecular dynamics of the collagen backbone in intact connective tissues has been investigated using ^{13}C NMR line shape analysis to measure [13]CO chemical shift anisotropy (CSA) by Torchia et al.[11] They used [1-^{13}C]glycine to label samples from various sources in order to investigate the effect of crosslinking and mineralization on the peptide backbone motion in the collagen fibril. In another report by Torchia et al.,[12] the amplitude of motional fluctuations in collagen in intact tissues and reconstituted fibres were determined using ^{13}C NMR relaxation time measurements. [2-^{13}C]glycine labelled samples were used and the relaxation of the corresponding methylene carbon was followed. In both cases,[11,12] it was assumed that protein backbone motions are primarily a consequence of reorientation about the long axis of the molecule.

This motional model of a collagen rod librating about its helix axis was questioned in reference [13]; since, considering the size of the collagen molecule and the presence of crosslinked molecules, motional amplitudes derived for the helix axis libration (up to 33°) were unusually high. An alternative geometry of motion was suggested, which is based on small-angle librations (i.e., restricted rotations) about internal bond directions (Figure 2).[13,14] This geometry of the motion was deduced based on the analysis of the motional averaging of anisotropic ^{13}C CSA and ^{2}H quadrupolar interactions. It was shown that the orthogonal orientation of the normal of the Gly amide plane relative to the libration axis leads to significant reduction of the ^{13}C CSA. The amplitude of libration depends on the number of torsional librations considered. For example, for collagen in mineralized calvaria the mono-axis libration of the torsional angle ψ(Gly) gives $\Phi = 9°$. However, considering the structure of collagen, a more realistic model must include librations about several ordinary bonds. For example, the penta-axes model including librations of torsional angles ψ(Gly), ϕ(Gly), ψ(Hyp), ϕ(Pro), and χ_4(Pro) in the Pro-Gly-Hyp triplet leads to $\Phi \leq 4°$.[13,15,16] Furthermore, it was shown that significant amplitude changes are observed over a narrow temperature range between $-18°C$ and $+18°C$, indicating that the dynamics of collagen is dependent on the state of the surrounding water.'[11–14] Reichert et al. have shown that by increasing the amount of water it is possible to induce larger amplitude motions of the protein atoms.[17–20] Studies of
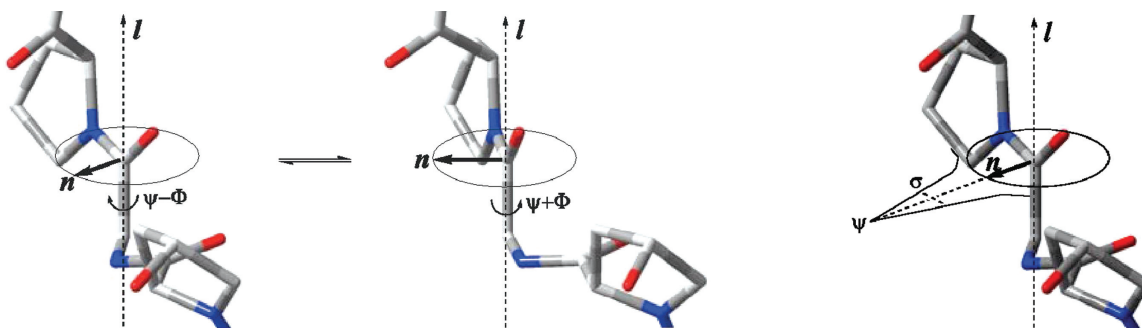

FIGURE 2 Internal bond libration about the C-C$^\alpha$ bond axis.[13] The normal (*n*) of the Gly plane is shown to librate: (a) about the bond axis (*l*) between either two sites with dihedral angles $\psi - \Phi$ and $\psi + \Phi$ or (b) about its averaged position corresponding to dihedral angle ψ with a Gaussian uncertainty σ.

lysozyme have also shown that water of hydration induces intramolecular motions in protein.[21,22]

In this work we intend to further investigate dependence of protein backbone and sidechain dynamics on the relative water content in collagen. In characterising this dependence, we will aim at quatifying the influence of water on protein motional amplitudes and frequencies. We will use solid-state ^{1}H and ^{13}C NMR measurements to follow the motional changes as a function of water content and temperature. Solid-state ^{13}C cross-polarization (CP) and magic angle spinning (MAS) NMR spectra will be measured to derive anisotropic chemical shift values, which then will be used to estimate changes in the motional amplitudes depending on temperature and water content. The theoretical background behind this type analysis is similar to that used for the analysis of ^{2}H quadrupolar parameters,[23–27] which have been employed widely for dynamics elucidations.[28–33] In addition to the ^{13}C CSA analysis, the selectivity of the [1]H-^{13}C dipolar dephasing MAS experiment will be exploited for comparing motional freedom of various amino acid carbon sites in collagen backbone and sidechain. The dependence of protein motional timescales on the water content will be examined using wideline ^{1}H NMR measurements.

EXPERIMENTAL

Materials and Equipment

Several samples containing collagen were used in this work. These were new parchment samples NP8 and SC81 produced according to traditional methods by craftsmen (received from Dr R. Larsen, Rector of School of Conservation, Copenhagen)[34] and collagen from bovine Achilles tendon (CBAT, received from Sigma-Aldrich). A typical amino acid distribution in % nmol in parchments is shown in Figure 1 of references [14] and [34].

Solid-state NMR experiments were carried out on a Bruker MSL300 spectrometer (7.05 T) in University College London and a Bruker AVANCE III 850 spectrometer (20 T) at the UK 850 MHz solid-state NMR facility at the University of Warwick.

Wideline ^{1}H NMR

A single-resonance Bruker probe with a 5 mm solenoid coil and short dead time characteristics was used for wideline ^{1}H NMR lineshape and T_2 measurements at 7.05 T. Typical 90° pulse length was in the range 1.7–2.2 μs and it was optimized for each sample studied. The recycle delay used in T_2-mesurements was 10 s. To measure short T_2 relaxation times, a simple

spin echo sequence, $90° - \tau - 180° - \tau$, was used, where 100 different τ echo delay values between 1.2 μs and 4 ms were used. The minimum τ used is limited by the hardware dead time. No pulse breakthrough effects or baseline distortions were observed at $\tau = 1.2$ μs or longer. For the deconvolution of ^{1}H NMR line shapes, a standard routine *mdcon* of XWINNMR (version 2.6) was used, which allows to use mixed Lorentzian/Gaussian line shapes.

Biexponential analysis of T_2-decay was carried using a Fortran program based on the simulated annealing algorithm.[35,36] The dependence of the intensities of the first points of FIDs on the echo delay τ was fitted to a sum of two exponentials as given by the following equation:

$$I = P^P \exp\left(-2\tau/T_2^P\right) + P^W \exp\left(-2\tau/T_2^W\right) \quad (1)$$

where τ is the echo delay, T_2^P and T_2^W are the corresponding T_2 values of the two components (protein and water), and P^P and P^W reflect relative amounts of the two components.

High-Resolution ^{13}C NMR

At 7.05 T, high-resolution solid-state ^{13}C were recorded using a standard 7 mm MAS probe (Bruker). At 20 T, high-resolution solid-state ^{13}C were recorded using a standard 4 mm MAS probe (Bruker). Parchments rolled into a cylindrical shape were fitted into zirconia rotors of 4 mm and 7 mm external diameters and spun at MAS frequencies in the range 1–14 kHz with stability better than ±3 Hz. High-resolution solid-state ^{13}C NMR spectra were recorded using cross-polarization (CP),[37,38] MAS and high-power ^{1}H decoupling. Typical acquisition conditions for ^{13}C CPMAS experiments at 7.05 T were: [1]H 90° pulse duration = 4 μs; contact time = 1.4 ms; recycle delay = 1.5–6 s; continuous wave ^{1}H decoupling. Typical acquisition conditions for ^{13}C CPMAS experiments at 20 T were: [1]H 90° pulse duration = 3.5 μs; contact time = 1 ms; recycle delay = 1.5–6 s; ^{1}H decoupling using the SPINAL-64 sequence.[39] The ^{1}H and ^{13}C chemical shifts are given relative to tetramethylsilane. The accuracy of the temperature controller used in this work was ±1 K and the long-term stability was better than ±0.5 K. Temperature calibration of the probe was done using the previously described procedure.[40]

Dipolar Dephasing

The dipolar dephasing experiment incorporates MAS, CP and ^{1}H decoupling and is mainly used for distinguishing signals because of quaternary and methyl carbons from methylene and methine carbons. However, it has also potential for molecular dynamics studies, which is explored in this work. A modified pulse sequence by Alemany et al.[41] was used in this work

for measurements of dipolar dephasing time constants (T_{dd}), which allows to acquire less distorted dipolar dephased spectra by introducing additional 180° pulses in the middle of the dipolar dephasing period t_{dd}. Using experiments with varying t_{dd}, the ^{13}C signal intensity changes were measured to derive T_{dd} values assuming the second-order exponential decay (Gaussian decay)[14,41]:

$$I = I_0 \exp\left(-t_{dd}^2/(T_{dd}^2)\right) \quad (2)$$

where I and I_0 are ^{13}C signal intensities with and without dipolar dephasing. At least 14 different values of the dipolar-dephasing delay (t_{dd}) between 1 μs and 50 μs were used. Note that the time constant T_{dd} in the above equation is equal to T_2 $\sqrt{2}$ of reference [41]. All T_{dd} measurements at both 7.05 T and 20 T were carried out at the MAS frequency of 4.4 kHz.

Chemical Shift Anisotropy

In a solid, molecules are present in all possible orientations with respect to the applied magnetic field, leading to a distribution of chemical shifts that gives rise to a broad signal called a powder pattern for a non-spinning sample. Analysis of the shape of the powder pattern allows the principal components (δ_{11}, δ_{22}, and δ_{33}) of the CSA to be determined. In the standard convention, the principal components of the CSA, δ_{11}, δ_{22}, and δ_{33}, are labelled according to the IUPAC rules.[42] The following relationships apply under this convention:

principal components $\delta_{11} \geq \delta_{22} \geq \delta_{33}$
isotropic chemical shift $\delta_{iso} = \frac{\delta_{11}+\delta_{22}+\delta_{33}}{3}$
span $\Omega = \delta_{11} - \delta_{33}$ ($\Omega \geq 0$).

Asymmetry parameter η defined under the Haeberlen–Mehring convention is useful for describing motional averaging of CSA together with the span Ω defined earlier. Under the Haeberlen–Mehring convention the asymmetry of CSA indicates by how much the line shape deviates from that of an axial symmetry. In the case of an axially symmetric CSA, $\eta = 0$. The following definitions are used under the Haeberlen-Mehring convention [43,44]:

principal components $|\delta_{zz}-\delta_{iso}| \geq |\delta_{xx}-\delta_{iso}| \geq |\delta_{yy}-\delta_{iso}|$
isotropic chemical shift: $\delta_{iso} = \frac{\delta_{xx}+\delta_{yy}+\delta_{zz}}{3}$
anisotropy $\Delta\sigma = \delta_{zz} - \frac{\delta_{xx}+\delta_{yy}}{2}$; asymmetry $\eta = \frac{\delta_{yy}-\delta_{xx}}{\delta_{zz}-\delta_{iso}}$, with $0 \leq \eta \leq 1$.

When the sample is subjected to MAS at a frequency that is less than the CSA, the powder pattern appears as a set of equally spaced narrow lines, comprising an isotropic peak and spinning sidebands. At slow MAS frequencies, the sideband

FIGURE 3 ^{13}C CPMAS NMR spectra of (a) NP8 dry, (b) NP8 with 12 wt% D$_2$O, (c) NP8 with 23 wt% D$_2$O, (d) NP8 with 31 wt% D$_2$O (recorded at 298 K, MAS frequency 4.4 kHz, external magnetic field strength 7.05 T). For full assignment of the ^{13}C peaks, see Figures 4 and 5 in reference [14].

intensity distribution can be used to obtain the principal components of the CSA.[45,46] The analysis of the motional averaging effects on individual CSA components is often used to deduce the geometry of the motion.[13,47–49] The procedure used to calculate the components of the motionally averaged CSA in the rapid motion regime and to determine the angular parameters that characterize the geometry of motion has been described previously.[13]

RESULTS AND DISCUSSION

Influence of Water on ^{13}C MAS NMR Lineshapes

^{13}C CPMAS spectra of NP8 "as received" and with different amounts of added heavy water are shown in Figures 3 and 4. No significant changes of peak positions were observed,
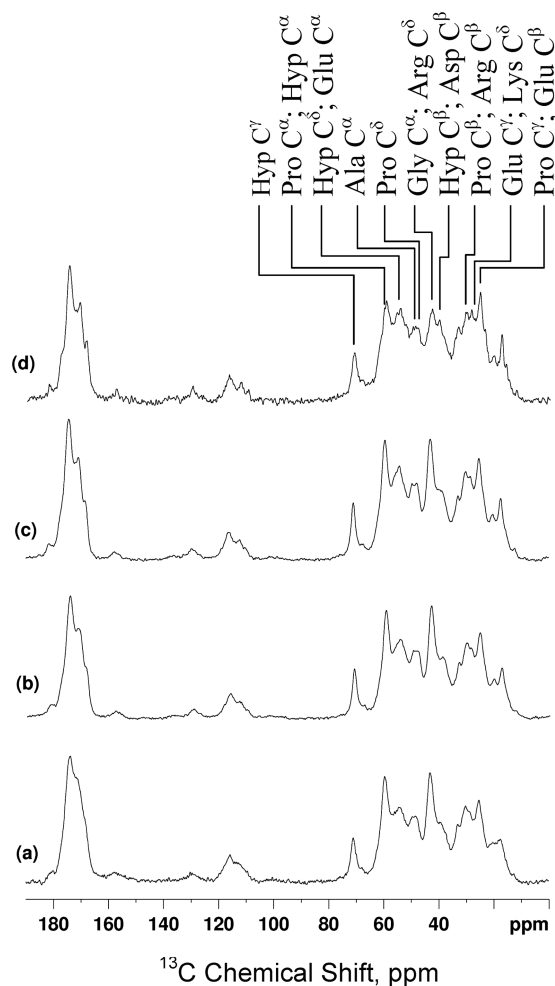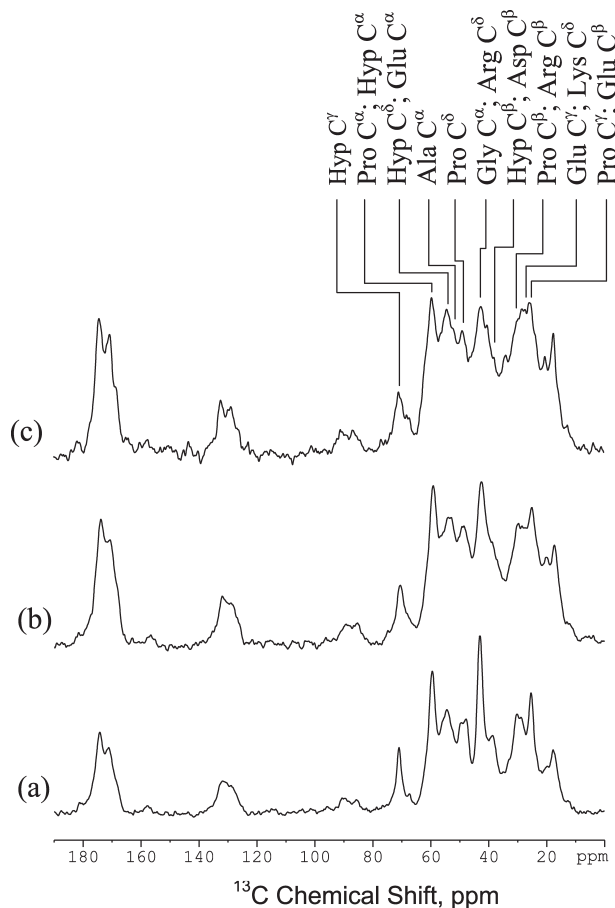
FIGURE 4 ^{13}C CPMAS NMR spectra of (a) NP8 dry, (b) NP8 with 14 wt% D$_2$O, (c) NP8 with 27 wt% D$_2$O (recorded at 298 K, MAS frequency 9 kHz, external magnetic field strength 20 T). For full assignment of the ^{13}C peaks, see Figures 4 and 5 in reference [14].

whereas the line widths of the peaks vary depending on the relative amount of added water. In particular, gradual decrease of line widths for the carbonyl (near ~175 ppm) and methyl carbons (near ~18 ppm, mainly due to the methyl carbon of Ala) is observed on increasing the water content. This is evident from the improved resolution of the peaks in these areas. Unlike the CH and CH$_2$ carbons, the C and CH$_3$ carbons are characterized by much smaller ^{1}H-^{13}C dipolar interactions due to larger distances from protons for the quaternary carbons and the methyl group rotation for the methyl carbons; hence, much smaller decoupling fields are needed for complete ^{1}H decoupling of these carbons. The line width changes for the CH and CH$_2$ carbons are less regular. For example, at 7.05 T the line widths of the peak at 43 ppm (mainly due to CH$_2$ of Gly) measured at 7/8th of its height were 95 Hz (0 wt% D$_2$O), 84 Hz (12 wt% D$_2$O), 91 Hz (23 wt% D$_2$O), 131 Hz (31 wt% D$_2$O), and 136 Hz (47 wt% D$_2$O). The increase of the line widths at very high contents of added D$_2$O (31–47 wt% D$_2$O)

can be attributed to the possibility of the interference of motions with frequencies of the order of the decoupling frequencies used (60–65 kHz).[50,51] This possibility was verified by measuring spectra of the (NP8 + 47 wt% D$_2$O) sample at two different decoupling fields (ν_D): 64 kHz and 96 kHz. The measured line widths of the peak at 43 ppm at 7/8th of its height were 136 Hz at ν_D = 64 kHz and 106 Hz at ν_D = 96 kHz. Narrower peaks at higher decoupling strength were also observed for other carbons. For example, the measured line widths of the peak at 25 ppm due to γ-CH$_2$ of Pro at 7/8th of its height were 67 Hz at ν_D = 64 kHz and 54 Hz at ν_D = 96 kHz. Although these preliminary observations are indicative of the dependence of collagen dynamics on its water content, they are not conclusive. Thus, further measurements of ^{13}C chemical shift anisotropy and ^{1}H-^{13}C dipolar dephasing rates were undertaken.

Changes in ^{13}C Chemical Shift Anisotropy as a Function of Temperature and Water Content

As shown previously,[11–14] the increase of the amplitude of fast reorientations with motional frequencies >10 kHz leads to a decrease of the span (Ω) of the ^{13}CO CSA in collagen samples. The results of our ^{13}CO CSA measurements using Herzfeld-Berger analysis of slow MAS spectra for various collagen containing samples are summarized in Table I. Despite the spectral overlap in this region, the measured ^{13}CO CSA changes in collagen are mainly due to the carbonyl groups of Gly, which constitutes one third of the amino acid residues, as well as other backbone carbonyls. Hence, by studying the changes in the motionally averaged values of the CSA the corresponding changes in the backbone dynamics can be followed.

First, we consider the results of our measurements for new parchment samples NP8 and SC81. From previous studies,[11–13] it is known that at ~253 K the backbone motion of collagen is frozen. We therefore measured the values of the CSA components at low temperatures in order to estimate the values of the CSA parameters (span, Ω, and asymmetry parameter, η) corresponding to a motionally static collagen molecules. At 233 K, the values of Ω and η for NP8 were 154.1 ± 0.7 ppm and 0.77 ± 0.01, respectively. The corresponding values at 295 K for NP8 are 150.1 ± 0.7 ppm and 0.77 ± 0.01. The small decrease of Ω on increasing the temperature suggests that the amplitude of motions involving peptide carbonyl at 295 K increases slightly compared with that at 233 K.

To quantify the changes in motional amplitudes as a function of temperature and the water content, we used a simple model of mono-axis motion and assumed that librational motion about the C-C$^\alpha$ bond is the major source of motional averaging. This is similar to the approach described previously

Table I The ^{13}CO CSA Components Determined from CPMAS Spectra Recorded at 1.75 kHz

Sample	T(K)	δ_{iso} (ppm)	$\delta_{11}-\delta_{iso}$ (ppm)	$\delta_{22}-\delta_{iso}$ (ppm)	$\delta_{33}-\delta_{iso}$ (ppm)	Ω (ppm)	η	Φ (°)	R^a (ppm)
NP8	233	173.9	72.4	9.3	−81.7	154.1	0.77	–	–
NP8	295	173.9	70.5	8.9	−79.6	150.1	0.77	7	0.08
NP8+12 wt%D$_2$O	295	174.0	69.8	9.1	−79.0	148.7	0.77	8	0.21
NP8+23 wt%D$_2$O	295	174.1	69.1	8.8	−78.0	147.0	0.77	10	0.18
NP8+31 wt%D$_2$O	295	174.4	67.7	7.0	−74.7	142.4	0.81	13	0.27
NP8+38 wt%H$_2$O	295	174.5	63.7	9.2	−72.9	136.6	0.75	15	0.92
SC81	295	173.9	70.7	9.4	−80.1	150.9	0.77	7	0.21
CBAT	295	174.0	68.3	8.6	−76.9	145.2	0.78	11	0.20

^{a} The merit function R (ppm) for the simulated annealing fittings of the ^{13}CO CSA for the determination of the librational amplitude Φ (°) is defined as $R = \sqrt{\frac{1}{3}\sum_{i=1}^{3}(\delta_{ii}^{exp}-\delta_{ii}^{calc})^2}$, where δ_{ii}^{exp} and δ_{ii}^{calc} are experimental and calculated CSA components. Estimated uncertainties in Ω, η and Φ values were ±0.7 ppm, ±0.01 and ±1°, respectively. Spectra with satisfactory signal-to-noise ratios were obtained in all cases. The main source of errors in the determined values arises from integral intensity determinations due to the signal overlap.

for the ^{13}C-labelled collagens.[13] Higher flexibility of the protein backbone about the C-C$^\alpha$ bond compared with other bonds is supported by the previous analysis in which the direction of the libration axis was derived from the CSA calculations of [1-^{13}C]-Gly labelled collagens.[13] As the static values, we used CSA values measured at 233 K (Table I). From the ^{13}CO CSA fittings using simulated annealing algorithm,[13,35,36] we determined the values of the librational amplitudes Φ. These are included in Table I. The changes in Φ values indicate that the increase of water content leads to a significant increase of the Φ value. For example, the value of Φ for NP8 was 7°, whereas the sample of NP8 containing 38 wt% of added H$_2$O showed Φ = 15°. Overall, the obtained results show that:

i. backbone dynamics collagen from bovine Achilles tendon (CBAT) and in parchments are significantly restricted compared to collagens studied previously, but similar to the mineralized collagen[13,17–20];

ii. addition of water (either H$_2$O or D$_2$O) to parchments leads to a significant increase of backbone motional amplitudes of collagen molecules.

Dependence of ^{1}H-^{13}C Dipolar Dephasing Rates on Temperature and Water Content

Tables II and III summarize the results of our T_{dd} measurements at 20 T and 7.05 T, respectively. As expected, T_{dd} values are higher at higher temperatures, reflecting the increase of the motional amplitudes on increasing the temperature. For example, in NP8 the T_{dd} value of the C$^\gamma$-H of Hyp is 38 μs at 213 K and 42 μs at 298 K at 20 T and ν_r = 4.4 kHz. At 7.05 T and ν_r = 4.4 kHz, the corresponding T_{dd} value of the C$^\gamma$-H of Hyp is 24 μs at 233 K and 26 μs at 298 K. The observed field dependence of T_{dd} has not been investigated, but it is likely that the

measured values depend on both the MAS frequency and the external field, that is, higher MAS frequencies at higher fields are needed in order to retain the T_{dd} value constant.

The dependence on the added water content can be followed from the T_{dd} values measured for NP8 and SC81 (Tables II and III). As in the case of the temperature dependence, the gradual increase of T_{dd} values with the increase of the amount of added water suggests the increase of the reorientational amplitudes.

By dividing the rigid value of T_{dd} determined at low temperatures by the motionally averaged values of T_{dd} at 298 K (Table IV) an order parameter $\mathcal{S}$ of the C-H bond can be determined, which is a dimensionless measure of the amplitude of the C-H reorientations. This parameter varies between 0 and 1, with higher values corresponding to motionally restricted cases with smaller reorientational amplitudes. For a simple two-site jump the order parameter is expected to depend on the populations of the sites (p_1 and p_2, with $p_1 + p_2$ = 1) and the jump angle Φ.[52,53] Note that a two-site jump model is suitable for the description of the Pro sidechain dynamics, as supported by NMR,[54–56] quantum-mechanical calculations[54,55] and MD simulations.[54,56,57]

For samples with no added water, the values of $\mathcal{S}$ for various ^{13}C sites in collagen at two different fields suggest that the most mobile part of the collagen molecule include the C-H bonds of the sidechain carbon sites resonating between 25 and 31 ppm (Tables (II–IV)). These are mainly the sidechain C-H bonds of Pro, Arg, Glu, and Lys residues in collagen (Figure 5). The addition of water leads to significant increase of motional amplitudes (i.e., jump angles) of all the measured C-H bond directions in collagen. From the average ratio of the $\mathcal{S}$ values for dry and wet samples, the increase in the motional amplitudes for the sidechain C-H bonds ($\mathcal{S}_{dry}/\mathcal{S}_{wet} \approx 1.53$) is

Table II The Values of T_{dd} (μs) and $\mathcal{S}$ from the Measurements at 20 T (MAS Frequency 4.4 kHz, at Ambient Probe Temperature, Unless Otherwise Indicated)[a]

δ_C (ppm)	Carbon	Type of Carbon	NP8 213 K T_{dd}/μs	NP8 T_{dd}/μs	NP8+14 wt% D$_2$O T_{dd}/μs	NP8 $\mathcal{S}$	NP8+14 wt% D$_2$O $\mathcal{S}$
71.1	Hyp C$^\gamma$	CH	38	42	46	0.90	0.83
59.6	Pro C$^\alpha$; Hyp C$^\alpha$	CH	38	41	44	0.93	0.86
54.3	Hyp C$^\delta$; Glu C$^\alpha$	CH	39	39	42	1.00	0.93
49.8	Ala C$^\alpha$	CH	39	39	42	1.00	0.93
47.8	Pro C$^\delta$	CH$_2$	34	35	39	0.97	0.87
43.2	Gly C$^\alpha$; Arg C$^\delta$	CH$_2$	32	34	38	0.94	0.84
38.9	Hyp C$^\beta$; Asp C$^\beta$	CH$_2$	37	38	43	0.97	0.86
30.5	Pro C$^\beta$; Arg C$^\beta$	CH$_2$	37	41	45	0.90	0.82
28.7	Glu C$^\gamma$; Lys C$^\delta$	CH$_2$	37	40	45	0.93	0.82
25.4	Pro C$^\gamma$; Glu C$^\beta$	CH$_2$	38	44	49	0.86	0.78

[a] The estimated uncertainties in T_{dd} values are within ± 1 μs. From measurements at two different fields, deviations in $\mathcal{S}$ values vary between ± 0.01 and ± 0.09. The main source of errors in these measurements is due to the signal overlap.

Table III The Results of T_{dd} (μs) Measurements at 4.4 kHz (at Ambient Probe Temperature, Unless Otherwise Indicated)[a]

Carbon	δ_C (ppm)	Type of carbon	NP8 233K	NP8	NP8 + 12 wt%D$_2$O	NP8 + 23 wt%D$_2$O	NP8 + 31 wt%D$_2$O	NP8 + 47 wt%D$_2$O	SC81+51 wt%H$_2$O	SC81	CBAT
Hyp C$^\gamma$	71.1	CH	24	26	29	33	36	37	37	26	29
Pro C$^\alpha$; Hyp C$^\alpha$	59.6	CH	24	25	28	31	34	35	36	25	28
Hyp C$^\delta$; Glu C$^\alpha$	54.3	CH	25	26	27	32	34	35	36	26	29
Ala C$^\alpha$	49.8	CH	23	24	26	31	34	35	34	25	27
Pro C$^\delta$	47.8	CH$_2$	21	22	24	29	31	33	33	23	25
Gly C$^\alpha$; Arg C$^\delta$	43.2	CH$_2$	19	20	22	25	28	29	31	19	22
Hyp C$^\beta$; Asp C$^\beta$	38.9	CH$_2$	20	22	23	28	31	33	34	22	24
Pro C$^\beta$; Arg C$^\beta$	30.5	CH$_2$	21	25	26	31	36	37	38	24	36
Glu C$^\gamma$; Lys C$^\delta$	28.7	CH$_2$	21	25	26	31	35	40	38	23	28
Pro C$^\gamma$; Glu C$^\beta$	25.4	CH$_2$	24	28	29	33	37	41	38	26	31

[a] The estimated uncertainties in T_{dd} values are within ± 1 μs. The main source of errors in these measurements is due to the signal overlap.

Table IV The Order Parameter $\mathcal{S}$ Calculated Using T_{dd} (μs) Values[a]

Carbon	δ_C (ppm)	Type of carbon	NP8 233K	NP8	NP8 + 12 wt%D$_2$O	NP8 + 23 wt%D$_2$O	NP8 + 31 wt%D$_2$O	NP8 + 47 wt%D$_2$O	SC81+51 wt%H$_2$O	SC81	CBAT
Hyp C$^\gamma$	71.1	CH	24	26	29	33	36	37	37	26	29
Pro C$^\alpha$; Hyp C$^\alpha$	59.6	CH	24	25	28	31	34	35	36	25	28
Hyp C$^\delta$; Glu C$^\alpha$	54.3	CH	25	26	27	32	34	35	36	26	29
Ala C$^\alpha$	49.8	CH	23	24	26	31	34	35	34	25	27
Pro C$^\delta$	47.8	CH$_2$	21	22	24	29	31	33	33	23	25
Gly C$^\alpha$; Arg C$^\delta$	43.2	CH$_2$	19	20	22	25	28	29	31	19	22
Hyp C$^\beta$; Asp C$^\beta$	38.9	CH$_2$	20	22	23	28	31	33	34	22	24
Pro C$^\beta$; Arg C$^\beta$	30.5	CH$_2$	21	25	26	31	36	37	38	24	36
Glu C$^\gamma$; Lys C$^\delta$	28.7	CH$_2$	21	25	26	31	35	40	38	23	28
Pro C$^\gamma$; Glu C$^\beta$	25.4	CH$_2$	24	28	29	33	37	41	38	26	31

[a] From measurements at two different fields for NP8, deviations in $\mathcal{S}$ values vary between ± 0.01 and ± 0.09. The main source of errors in these measurements arises from the signal overlap.
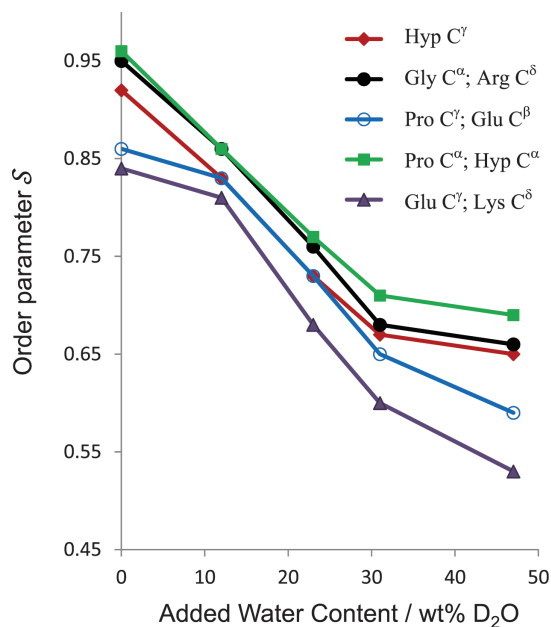
FIGURE 5 The order parameter $\mathcal{S}$ of various sites in collagen in NP8 at varying amounts of added D_2O at 298 K. The estimated uncertainties in the order parameter $\mathcal{S}$ were ± 0.02 (Hyp C^γ), ± 0.02 (Gly C^α; Arg C^δ), ± 0.05 (Pro C^γ; Glu C^β), ± 0.03 (Pro C^α; Hyp C^α), and ± 0.09 (Glu C^γ; Lys C^δ).

FIGURE 6 Experimental ^{1}H NMR spectra of NP8 (a) "as received" sample; (b) NP8 soaked in D_2O for 1 hour (contains 79.4 wt% D_2O).

slightly higher than that for the backbone ($\mathcal{S}_{dry}/\mathcal{S}_{wet} \approx 1.40$). Overall, the order parameters determined in this work are in good agreement with those measured directly through the detection of motionally averaged dipolar couplings as a function of hydration by Reichert et al.[17] and Zernia and Huster.[19] Slightly smaller values of $\mathcal{S}$ measured in this work compared to those measured by Reichert et al.[17] for CBAT may be caused by the higher water content in parchments. We note that in the CBAT sample used in this work additional lipid impurities (with the alkane chain C_nH_{2n+1}) were detected in ^{13}C CPMAS spectra,[58] the overlap of which with the collagen peaks in the aliphatic area is expected to lead to less accurate values of the order parameters. No lipid or other impurities were found in parchments used in this work.

Using T_{dd}^{-1} as a quantity proportional to ^{1}H-^{13}C dipolar couplings, we can analyze the motional averaging T_{dd}^{-1} in a manner similar to that used for the analysis of ^{2}H quadrupolar couplings[25] or ^{13}C CSAs[13] in the fast exchange region. As before,[13] we consider a mono-axis two-site jump model which allows to determine the upper limit estimates of Φ. As the rigid value of T_{dd} at 7.05 T we use 19 μs, which is the same for the Gly methylene group of NP8 at 233 K (Table III) and that of glycine at 203 K. From the T_{dd} value of Gly C^α in NP8 with no added water (Table III), the upper limit estimate of Φ under the two-site mono-axis model (e.g., restricted rotation about the C-C^α bond, Figure 2a)[13] is 11°
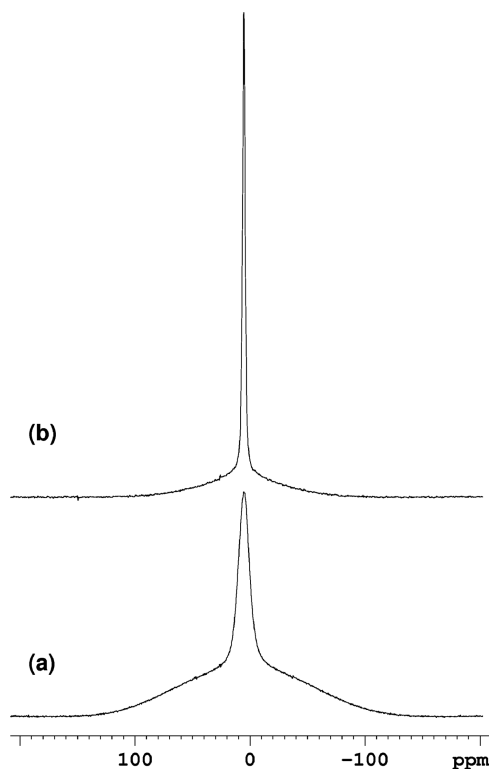
at 298 K. Similarly, the upper limit estimates of Φ were 19° (12 wt%D_2O), 25° (23 wt%D_2O), 29° (31 wt%D_2O) and 31° (47 wt% D_2O). Despite the simplicity of the model considered, these results suggest that the increase of the water content could lead to significant increase of the internal restricted rotations (i.e., librations) about C-C^α or N-C^α bonds of the collagen backbone. Overall, the observed dependence of collagen dynamics on the water content is in agreement with the previous reports,[11–13,17–20,59–62] as well as the results of studies on the effect of hydration of the molecular mobility of collagen in bone and cartilage.[18–20,59–62] The dependence of collagen dynamics on the water surrounding appears to be its intrinsic property, which is retained in different environments in the presence of lipids, calcium phosphate, glycosaminoglycans, and other species.

Wideline ^{1}H NMR Lineshape Changes

Figure 6a illustrates wideline spectrum of NP8 recorded at room temperature. The wideline spectrum is a superposition of two peaks with considerably different line widths. The narrow peak in this spectrum is attributed to the bound (structural) water protons and the broad peak is attributed to the collagen protons.

The large difference in the line widths of two peaks allowed us to use line shape fittings to derive peak areas and line widths corresponding to these peaks. The results of the line shape fitting showed that the ratio (P^W/P^P) of the water (P^W) and protein (P^P) peak areas was 0.354. Using the known amino acid distribution in parchments[34] and the P^W/P^P ratio of 0.354, the initial H_2O content can be evaluated as ~15 wt% in NP8. From the line shape fittings, the line widths of the water (L^W) and protein (L^P) peaks were 3.370 ± 0.002 kHz and 38.08 ± 0.02 kHz, respectively. Large differences in line widths of the two peaks indicate that corresponding spin-spin relaxation times (T_2) are different and that the T_2 value for the broad peak is likely to be very short (see below).

[1]H spectra of NP8 with 79.4 wt% D_2O is shown in Figure 6b. As can be seen, significant narrowing of both narrow and broad peaks occurs on adding D_2O. However, no sharp peak with a linewidth of ~100 Hz or less is observed, which can be attributed to H_2O or HOD molecules in a liquid like phase. The best fit values L^W and L^P for the sample containing 79.4 wt% D_2O were 0.709 ± 0.001 kHz and 23.71 ± 0.05 kHz, respectively. As T_2 is inversely proportional to L, this result already suggests that the relaxation times T_2 for both water and protein molecules are significantly increased in the presence of D_2O.

Relaxation times are good indicators of the motional changes and the correlation times can be estimated using T_2 relaxation times. For the analysis of the protein T_2 data, a simplified Lipari-Szabo model can be used.[53] Under the Lipari-Szabo formalism, the spectral density is defined as:

$$J(\omega) = \frac{S^2 \tau_c}{1 + (\omega_L \tau_c)^2} + \frac{(1-S^2)\tau_{tot}}{1 + (\omega_L \tau_{tot})^2} \quad (3)$$

$$(\tau_{tot})^{-1} = (\tau_c)^{-1} + (\tau_e)^{-1} \quad (4)$$

where τ_c is the correlation time for the overall molecular motion and τ_e is an effective correlation time for the internal motions. In the case of collagen, the overall correlation time τ_c approaches infinity[53,63] and Eq. (3) simplifies into:

$$J(\omega) = \frac{(1-S^2)\tau_e}{1 + (\omega_L \tau_e)^2} \quad (5)$$

Under this simplified Lipari Szabo model, it is assumed that the internal motion can be approximated using a single correlation time τ_e. The T_2 relaxation time of protein protons can then be calculated using the following equation:[64]

$$\frac{1}{T_2} = \frac{3}{20} \frac{\gamma_H^4 \hbar^2}{r_{ij}^6} \left(\frac{\mu_0}{4\pi}\right)^2 [3J(0) + 5J(\omega_L) + 2J(2\omega_L)] \quad (6)$$

Table V Proton T_2 Relaxation Times and Estimated Internal Correlation Times τ_e in NP8 Samples Containing D_2O[a]

wt % D_2O	T_2 (μs)	S[b]	τ_e (μs)
79.4	36.4	–	–
66.8	31.2	–	–
55.7	29.6	–	–
45.0	27.0	0.66	8
33.3	22.5	0.68	10
19.8	18.4	0.76	15
9.8	16.0	0.86	28
0	9.7	0.95	123

[a] Estimated uncertainties in T_2 and τ_e values are ±0.8 μs and ±2 μs. The main source of errors is due to the overlap of the water and protein signals.
[b] The values of S at 0, 9.8, 19.8, 33.3 and 45 wt%D_2O are assumed to be equal to those in Table IV at 0, 12, 23, 31, and 47 wt%D_2O, respectively.

The results of T_2 measurements using the Hahn echo sequence are included in Table V for NP8 samples containing different amounts of D_2O. The internal correlation times of protein molecules (τ_e) shown in Table V were calculated using Eqs. (5) and (6). The above determined values of order parameter S (Table IV) for the Gly residue were used in τ_e calculations with the water content between 0 and 45 wt% D_2O, as glycine is the most abundant residue in collagen and constitutes one third of all the amino acid residues. In these calculations, we have assumed that only short-range interactions are important, as T_2 is proportional to r_{ij}^6. Thus, the interproton distance of 1.76 Å was used for the glycine CH_2 groups of collagen. The values of τ_e estimated in this manner (Table V) suggest that motional frequencies of protein gradually increase as the amount of D_2O is increased. Combined with the results of the CSA and dipolar dephasing measurements, we can conclude that both the frequency and the amplitude of protein motions are increased significantly on increasing the D_2O content.

CONCLUDING REMARKS

In line with previous reports,[11–14,17–20,59–62] our solid-state NMR studies of collagen samples of various origin confirm that the amplitude of collagen backbone and sidechain motions increases significantly on increasing the water content. This conclusion is supported by the changes observed in three different in nature NMR observables: (i) the linewidth dependence on the ^{1}H decoupling frequency; (ii) ^{13}C CSA changes for the peptide carbonyl groups, and (iii) [1]H-^{13}C dipolar dephasing rates. Considering the NMR observables involved, the timescale of the protein motions dependent on the added water content can be estimated to be of the order of microseconds. This estimate agrees with that from our wideline proton T_2 NMR measurements. In addition, our wideline ^{1}H NMR

measurements show that the timescale of the microsecond motions in proteins reduces significantly on increasing the added water content. In particular, an ~15-fold increase in protein motional frequencies is observed on increasing the added water content to 45 wt% D_2O. A nearly three-fold increase in motional amplitudes of the backbone librations about C-C$^\alpha$ or N-C$^\alpha$ bonds is also found on increasing the added water content to 47 wt% D_2O.

We note that structural water molecules were present in collagen samples before addition of water in our experiments.[14] A simple model that would agree with the observed changes in collagen dynamics must therefore include the exchange of structural and added water molecules as a result of increased water translational diffusion of water molecules on increasing its content. The structural water forming a scaffold around the triple-helix is known to stabilize collagen's higher order structure by forming hydrogen bonds with polar functionalities of peptides. To a degree, hydrogen-bonded water molecules can therefore be considered as extended sidechains of proteins. Their exchange with the free water molecules as a result of translational diffusion would involve the breakage and formation of new hydrogen bonds with protein and is therefore likely to cause changes in the motional amplitudes and frequencies of the protein sidechain and backbone, as revealed by solid-state NMR measurements. Note that evidence in favour of the translational diffusion of water molecules on protein surface has also been provided by incoherent quasielastic neutron scattering (IQNS) studies.[22] It was shown that water molecules of the first hydration layer of the crystalline hen egg-white lysozyme, as well as those of the second incomplete hydration layer confined between protein molecules diffuse translationally.[22] Further computational studies are currently underway in order to gain a better insight into the dependence of protein dynamics on surrounding water molecules.

REFERENCES

1. Fratzl, P. Collagen Structure and Mechanics; Springer-Verlag: New York, 2008.
2. Ramachandran, G. N. Int J Pept Protein Res 1988, 31, 1–16.
3. Ramachandran, G. N.; Ramakrishnan, C. In Biochemistry of Collagen; Ramachandran, G. N., Reddi, A. H., Eds.; Plenum Press: New York, 1976; pp 45–84.
4. Ramachandran, G. N. In Treatise on Collagen; Ramachandran, G. N., Ed.; Academic Press: New York, 1967; pp 102–183.
5. Okuyama, K.; Miyama, K.; Morimoto, T.; Masakiyo, K.; Mizuno, K.; Bächinger, H. P. Biopolymers 2011, 95, 628–640 (references therein).
6. Traub, W.; Piez, K. A. Adv Protein Chem 1971, 25, 243–352.
7. Gelman, R. A., Williams, B. R.; Piez, K. A. J Biol Chem 1979, 254, 180–186.
8. Berisio, R.; Vitagliano, L.; Mazzarella, L.; Zagari, A. Protein Sci 2002, 11, 262–270.
9. Kramer, R. Z.; Bella, J.; Mayvile, P.; Brodsky, B.; Berman, H. M. Nat Struct Biol 1999, 6, 454–457.
10. Privalov, P. L. Adv Prot Chem 1982, 35, 1–104.
11. Sarkar, K.; Sullivan, C. E.; Torchia, D. A. J Biol Chem 1983, 258, 9762–9767.
12. Sarkar, K.; Sullivan, C. E.; Torchia, D. A. Biochemistry 1985, 24, 2348–2354.
13. Aliev, A. E. Chem Phys Lett 2004, 398, 522–525.
14. Aliev, A. E. Biopolymers 2005, 77, 230–245.
15. Molecular dynamics simulations are in agreement with the geometry of the motion deduced from solid-state NMR (Figure 2).[13,14] For a model collagen 1K6F (with Pro^1-Gly-Pro^2 triplets) placed in an environment similar to that in collagen fibrils,[8] a 235 ns long MD trajectory calculated using the AMBER99SB force field[16] shows large variations in torsional angles for amino acid residues in the middle of the peptide chain: $\psi(\text{Gly}) = 172 \pm 10°$, $\varphi(\text{Gly}) = -70 \pm 9°$, $\psi(\text{Pro}^1) = 147 \pm 9°$, $\varphi(\text{Pro}^1) = -59 \pm 9°$, $\psi(\text{Pro}^2) = 152 \pm 8°$, $\varphi(\text{Pro}^2) = -65 \pm 10°$, $\chi_2(\text{Pro}^1) = 13 \pm 29°$ and $\chi_2(\text{Pro}^1) = 0 \pm 31°$. These variations of the backbone torsions in MD simulations and the librational amplitudes predicted by the solid-state NMR analyses are of similar magnitude.[13,14,17–20] Full details of MD simulations will be presented in a forthcoming paper.
16. Hornak, V.; Abel, R.; Okur, A.; Strockbine, B.; Roitberg, A.; Simmerling, C. Prot Struct Funct Bioinfo 2006, 65, 712–725.
17. Reichert, D.; Pascui, O.; de Azevedo, E. R.; Bonagamba, T. J.; Arnold, K.; Huster, D. Magn Reson Chem 2004, 42, 276–284.
18. Huster, D.; Schiller, J.; Arnold, K. Magn Reson Med 2002, 48, 624–632.
19. Zernia, G.; Huster, D. NMR Biomed 2006, 19, 1010–1019.
20. Förster, P. A.; Scheidt, H. A.; Hacker, M. C.; Schulz-Siegmund, M.; Ahnert, P.; Schiller, J.; Rammelt, S.; Huster, D. Magn Reson Med 2012; doi:10.1002/mrm.24541.
21. Rupley, J. A.; Careri, G. Adv Prot Chem 1991, 41, 37–172.
22. Bon, C.; Dianoux, A. J.; Ferrand, M.; Lehmann, M. S. Biophys J 2002, 83, 1578–1588.
23. Griffin, R. G. Meth Enzymol 1981, 72, 108–174.
24. Alam, T. M.; Drobny, G. P. Chem Rev 1991, 91, 1545–1590.
25. Wittebort, R. J.; Olejniczak, E. T.; Griffin, R. G. J Chem Phys 1987, 86, 5411–5420.
26. Hoatson, G. L.; Vold, R. L. NMR Basic Principles and Progress, Vol. 32, Springer-Verlag: Berlin; 1994, pp 3–67.
27. Aliev, A. E.; Harris, K. D. M. Struct Bonding, 2004, 108, 1–53.

28. Ripmeester, J. A.; Ratcliffe, C. I. In Inclusion Compounds, Attwood, J. L.; Davies, J. E. D.; MacNicol, D. D., Eds.; Oxford University Press: Oxford, 1991; Vol. 5, 37–85.

29. Aliev, A. E.; Harris, K. D. M.; Shannon, I. J.; Glidewell, C.; Zakaria, C. M.; Schofield, P. A. J Phys Chem 1995, 99, 12008–12015.

30. Aliev, A. E.; Smart, S. P.; Shannon, I. J.; Harris, K. D. M. J Chem Soc Faraday Trans 1996, 92, 2179–2185.

31. Aliev, A. E.; Harris, K. D. M. J Phys Chem A 1997, 101, 4541–4547.

32. Cutajar, M.; Ashbrook, S. E.; Wimperis, S. Chem Phys Lett 2006, 423, 276–281.

33. Hogg, N. H. M.; Boulton, P. J. T.; Zorin, V. E.; Harris, R. K.; Hodgkinson, P. Chem Phys Lett 2009, 475, 58–63.

34. Larsen, R., Ed. Microanalysis of Parchment; Archetype Publications: London, 2002.

35. Press, W. H.; Flannery, B. P.; Teukolsky, S. A. Numerical Recipes in FORTRAN: the Art of Scientific Computing; Cambridge University Press, Cambridge, 1992.

36. Aliev, A. E.; Harris, K. D. M. Magn Reson Chem 1998, 36, 855–868.

37. Pines, A.; Gibby M.; Waugh, J. S. J Chem Phys 1973, 59, 569–590.

38. Schaefer, J.; Stejskal E. O.; Buchdahl, R. Macromolecules 1977, 10, 384–405.

39. Fung, B. M.; Khitrin, A. K.; Ermolaev, K. J Magn Reson 2000, 142, 97–101.

40. Aliev, A. E.; Harris, K. D. M. Magn Reson Chem 1994, 32, 366–369.

41. Alemany, L. B.; Grant, D. M.; Alger, T. D.; Pugmire, R. J. J Am Chem Soc 1983, 105, 6697–6704.

42. Sheppard, N.; Elyashévich, M. A.; Miller, F. A.; Becker, E. D.; Beynon, J. H.; Fluck, E.; Hadni, A.; Zerbi, G.; Herzberg, G.; Jeowska-Trzebiatowska, B.; Morino, Y.; Nagakura, S.; Rao, C. N. R.; Thompson, H.; Turner, D. W. Pure Appl Chem 1976, 45, 217–220.

43. Haeberlen, U. In Advances in Magnetic Resonance, Suppl. 1; Waugh, J. S., Ed.; Academic Press: New York, 1976.

44. Mehring, M. Principles of High Resolution NMR in Solids, 2nd ed.; Springer Verlag: Berlin, 1983.

45. Herzfeld, J.; Berger, A. E. J Chem Phys 1980, 73, 6021–6030.

46. Eichele, K.; Wasylishen, R. E. The program packages HBA was used: HBA 1.6.14. Dalhousie University and Universität Tübingen, Halifax (Canada), 2010.

47. Saito, H.; Ando, I.; Ramamoorthy, A. Prog Nucl Magn Reson Spectrosc 2010, 57, 181–228.

48. Lee, D. K.; Wittebort, R. J.; Ramamoorthy, A. J Am Chem Soc 1998, 120, 8868–8874.

49. Aliev, A. E.; Harris, K. D. M.; Champkin, P. H. J Phys Chem B 2005, 109, 23342–22350.

50. Rothwell, W. P.; Waugh, J. S. J Chem Phys 1981, 74, 2721–2732.

51. Kitchin, S. J.; Harris, K. D. M.; Aliev, A. E. Chem Phys Lett 2000, 323, 490–497 and references therein.

52. Mádi, Z. L.; Griesinger, C.; Ernst R. R. J Am Chem Soc 1990, 112, 2908–2914.

53. Lipari, G.; Szabo, A. J. Am Chem Soc 1982, 104, 4546–4559.

54. Aliev, A. E.; Courtier-Murias, D. J Phys Chem B 2007, 111, 14034–14042.

55. Aliev, A. E.; Bhandal, S.; Courtier-Murias, D. J Phys Chem A 2009, 113, 10858–10865.

56. Aliev, A. E.; Courtier-Murias, D.; Bhandal, S.; Zhou, S. Chem Commun 2010, 46, 695–697.

57. Aliev, A. E.; Courtier-Murias, D. J Phys Chem B 2010, 114, 12358–12375.

58. Ghioni, C.; Hiller, J. C.; Kennedy, C.J.; Aliev, A.E.; Odlyha, M.; Boulton, M.; Wess, T.J. J Lipid Res 2005, 46, 2726–2734.

59. Zhu, P.; Xu, J.; Sahar, N.; Morris, M. D.; Kohn, D. H.; Ramamoorthy, A. J Am Chem Soc 2009, 131, 17064–17065.

60. Xu, J.; Zhu, P.; Gan, Z.; Sahar, N.; Tecklenburg, M.; Morris, M. D.; Kohn, D. H.; Ramamoorthy, A. J Am Chem Soc 2010, 132, 11504–11509.

61. Xu, J.; Zhu, P.; Morris, M. D.; Ramamoorthy, A. J Phys Chem B 2011, 115, 9948–9954.

62. Mroue, K. H.; MacKinnon, N.; Xu, J.; Zhu, P.; McNerny, E.; Kohn, D. H.; Morris, M. D.; Ramamoorthy, A. J. Phys Chem B 2012, 116, 11656–11661.

63. Cole, H. B. R.; Torchia, D. Chem Phys 1991, 158, 271–281.

64. Harris, R. K. Nuclear Magnetic Resonance Spectroscopy; Longman Scientific and Technical: England, 1986.

Reviewing Editor: David E. Wemmer